Metascatter: Unifying Symbiotic Radio and Intelligent Reflecting Surface

Yang Zhao

Department of Electrical and Electronic Engineering
Imperial College London

Group Presentation, March 31, 2022

Table of Contents

Backscatter Communication

Backscatter allows wireless nodes to communicate without active RF chains on the tag.

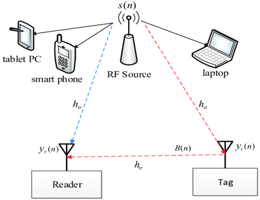

(a) AmBC [1]

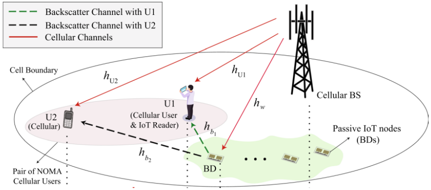

(b) SR [2]

- **Ambient Backscatter Communication (AmBC)** enables two battery-free devices to communicate over surrounding RF signals.
- **Symbiotic Radio (SR)** also involves transmit and/or receive cooperation.

Passive Beamforming

Backscatter also enables real-time adaptive channel reconfiguration using metamaterial.

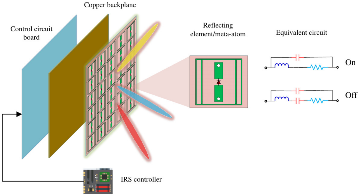

(a) IRS architecture [3]

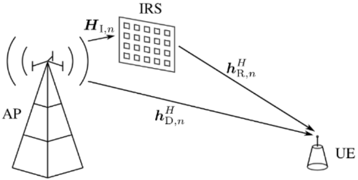

(b) IRS application [4]

- **Intelligent Reflecting Surface (IRS)** controls the scattering properties of passive reflecting elements.

Properties of Backscatter Systems

SR:

- Enable battery-less transmission over legacy systems
- Share spectrum, energy and infrastructures
- Achieve flexible primary-backscatter tradeoff

IRS:

- Enable real-time adaptive channel reconfiguration for legacy systems
- Involve massive reflection that benefits from array processing
- Achieve high passive beamforming gain

Name	BackCom	IRS	AmBC	SR
Coexisting systems (relationship)	1	1	2 (competitive)	2 (collaborative)
Transmitter role	Carrier emitter	Source	Carrier emitter	Source and carrier emitter
Backscatter contribution	Modulation	Channel control	Modulation	Modulation and channel uncertainty
Spectrum and energy sharing	No	No	Yes	Yes
Transceive cooperation	–	–	Neither	Both
Operation range	Medium	Long	Short	Short
Backscatter detection	Coherent	–	Non-coherent	Coherent (typically SIC)

Tag Structure

Passive tags harvest energy from and modulate information over incident signal.

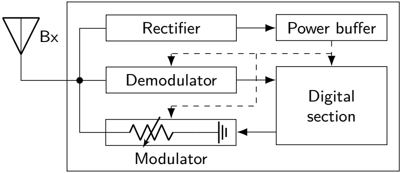

(a) Passive tag structure

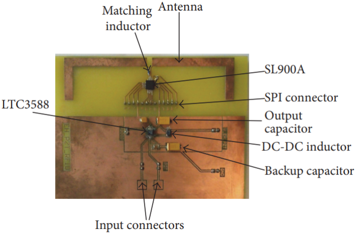

(b) RFID tag with energy harvesting module [5]

Backscatter Model

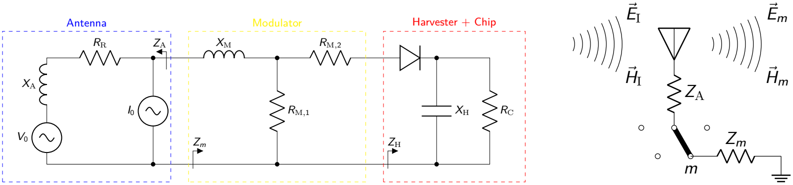

(a) Tag equivalent circuit

(b) Backscatter model

The complex reflection coefficient depends on the antenna-load impedance matching

$$\Gamma_m \triangleq \frac{Z_m - Z_{\mathrm{A}}^*}{Z_m + Z_{\mathrm{A}}}, \tag{1}$$

which controls the amplitude and phase of the backscatter signal.

Reflection Coefficient

SR varies the reflection coefficient for backscatter modulation

$$\Gamma_m = \alpha \frac{c_m}{\max_{m'} |c_{m'}|}. \tag{2}$$

IRS chooses the best reflection coefficient for passive beamforming

$$\Gamma_m = \beta_m \exp(j\theta_m). \tag{3}$$

Question

For a given reflector, is it possible to merge SR and IRS by proper reflection coefficient selection?

Table of Contents

Metascatter tags

Metascatter adapts the probability distribution of tag states to unify backscatter modulation and passive beamforming.

If all CSI can be estimated,

- IRS chooses the best state with probability 1
- SR assumes all input letters are equiprobable
- Metascatter enables flexible input design

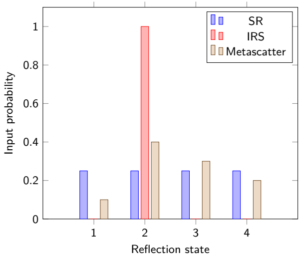

Figure: Tag probability distribution.

Metascatter System

Assume the backscatter pattern of all tags change per $N \gg 1$ primary symbols.

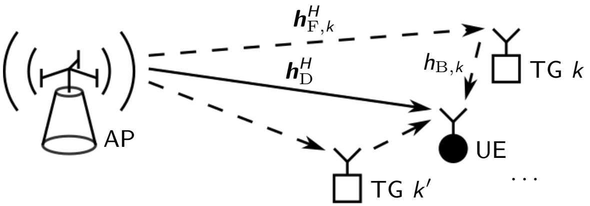

Figure: The proposed Metascatter system.

The received signal is

$$y[n] = \underbrace{\left(\boldsymbol{h}_{\mathrm{D}}^{H} + \sum_{k \in \mathcal{K}} \sqrt{\alpha_k} \boldsymbol{h}_{\mathrm{C},k}^{H} x_k \right)}_{\boldsymbol{h}_{\mathrm{E}}^{H}(x_{\mathcal{K}})} \boldsymbol{w} s[n] + w[n]. \tag{4}$$

Metascatter Decoding

We first jointly and non-coherently decode all backscatter symbols. The accumulated energy z over N primary symbol duration follows Erlang distribution

$$f(z \mid \mathcal{H}_{m_{\mathcal{K}}}) = \frac{z^{N-1} e^{-z/\sigma^2_{m_{\mathcal{K}}}}}{\sigma^{2N}_{m_{\mathcal{K}}} (N-1)!} \tag{5}$$

The backscatter decoding involves decision region threshold design over z.

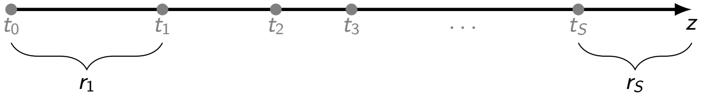

Figure: Decision region for each letter may contain disjoint partitions.

Metascatter Decoding

The transition probability from channel input $x_{m_{\mathcal{K}}}$ to output $\hat{x}_{m'_{\mathcal{K}}}$ is

$$P(\hat{x}_{m'_{\mathcal{K}}} \mid x_{m_{\mathcal{K}}}) = \int_{\mathcal{R}_{m'_{\mathcal{K}}}} f(z \mid \mathcal{H}_{m_{\mathcal{K}}}) \mathrm{d}z. \tag{6}$$

Once successfully recovered, the backscatter symbols are modeled within equivalent channel for primary decoding.

Achievable Rates

Denote the input probability of tag k at state m_k as $P_k(x_{m_k})$, and the probability of input combination $x_{m_\mathcal{K}}$ as $P_\mathcal{K}(x_{m_\mathcal{K}}) = \prod_{k\in\mathcal{K}} P_k(x_{m_k})$ (independent encoding).

The backscatter achievable rate is

$$I_\mathrm{B}(x_\mathcal{K}; \hat{x}_\mathcal{K}) = \sum_{m_\mathcal{K}} P_\mathcal{K}(x_{m_\mathcal{K}}) \sum_{m'_\mathcal{K}} P(\hat{x}_{m'_\mathcal{K}} \mid x_{m_\mathcal{K}}) \log \frac{P(\hat{x}_{m'_\mathcal{K}} \mid x_{m_\mathcal{K}})}{P(\hat{x}_{m'_\mathcal{K}})}. \tag{7}$$

The primary (ergodic) rate is

$$I_\mathrm{P}(x_\mathcal{K}; \boldsymbol{y}) = \sum_{m_\mathcal{K}} P_\mathcal{K}(x_{m_\mathcal{K}}) N \log_2 \left(1 + \frac{|\boldsymbol{h}_\mathrm{E}^H(x_{m_\mathcal{K}})\boldsymbol{w}|^2}{\sigma_w^2}\right). \tag{8}$$

The achievable rates depend on tag input distribution, energy decision threshold, and transmit precoder design.

Optimization Problem

We aim to characterize the primary-(sum-)backscatter rate region.

$$\max_{\{\boldsymbol{p}_k\},\boldsymbol{t},\boldsymbol{w}} \quad I(x_{\mathcal{K}}; \hat{x}_{\mathcal{K}}, \boldsymbol{y}) \triangleq \rho I_{\mathrm{P}}(x_{\mathcal{K}}; \boldsymbol{y}) + (1-\rho) I_{\mathrm{B}}(x_{\mathcal{K}}; \hat{x}_{\mathcal{K}}) \tag{9a}$$

$$\text{s.t.} \quad \sum\nolimits_{m_k} P_k(x_{m_k}) = 1, \quad \forall k \in \mathcal{K}, \tag{9b}$$

$$P_k(x_{m_k}) \geq 0, \quad \forall k \in \mathcal{K}, \ \forall m_k \in \mathcal{M}, \tag{9c}$$

$$\|\boldsymbol{w}\|^2 \leq P. \tag{9d}$$

Since problem (9) is not jointly convex, we propose a BCD algorithm that iteratively updates $\{\boldsymbol{p}_k\}$, $\boldsymbol{t}$ and $\boldsymbol{w}$ until convergence.

Input Probability Distribution

For a given threshold and precoder, the input distribution design is non-convex when $K > 1$.

- GP needs to approximate $\prod_{k \in \mathcal{K}} P_k(x_{m_k}) \log \prod_{k \in \mathcal{K}} P_k(x_{m_k})$ with high complexity
- SCA and KKT solutions are trapped at saddle points

KKT Solution

The KKT solution is given by the converging point of the sequence

$$P_k^{(r+1)}(x_{m_k}) = \frac{P_k^{(r)}(x_{m_k}) \exp\left(\frac{\rho}{1-\rho} I_k^{(r)}(x_{m_k}; \hat{x}_{\mathcal{K}}, \boldsymbol{y})\right)}{\sum_{m_k'} P_k^{(r)}(x_{m_k'}) \exp\left(\frac{\rho}{1-\rho} I_k^{(r)}(x_{m_k'}; \hat{x}_{\mathcal{K}}, \boldsymbol{y})\right)}, \tag{10}$$

where r is the iteration index and $\boldsymbol{p}_k^{(0)} > \boldsymbol{0}$, $\forall k \in \mathcal{K}$.

Transmit Precoder

The optimal precoder design is highly non-convex that involves integration, entropy term, and variable on exponential. We may propose a suboptimal precoder based on linear combination of equivalent and cascaded channels, or consider single transmit antenna instead.

Decision Threshold

Once the input distribution is determined, (6) becomes a point-to-point channel since total backscatter rate is considered.

Minimum Number of Thresholds

The minimum number of distinct thresholds for problem (9) is $L+1$ if there are L input combinations with non-zero probability.

Table of Contents

System Model

[6] aims to obtain the optimal M-level quantizer for DMC with q inputs and N outputs.

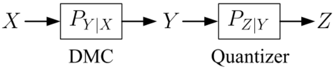

Figure: Quantization of DMC [6]

Essentially, the continuous output is discretized into N fine-grained bins.

Quantization cost

Preliminary:

- There exists a deterministic quantizer that is optimal
- The optimal quantizer is convex w.r.t. backward channel $P(X|Y)$

The cost of quantizing $\{y_l, \dots, y_r\}$ into one level is

$$w(l, r) = \sum_{j'=l}^{r} P_Y(y_{j'}) \phi \left(\frac{\sum_{j=l}^{r} P_{X,Y}(\cdot, y_j)}{\sum_{j''=l}^{r} P_Y(y_{j''})} \right). \quad (11)$$

Dynamic Programming

The aim is to minimize the sum cost of allocating N bins to M letters.

It can be simplified by considering subproblem, to quantize $n < N$ bins into $m < M$ letters.

The core idea is to bridge the optimal cost function of subproblems when m increases, and shrink the search range based on existing results.

SMAWK

SMAWK algorithm [7] is designed to find the minimum value in each row of a monotone matrix. It can accelerate DP if the problem satisfies some nice properties.

Two reductions are applied alternately and recursively:

- Interpolate (when more rows or equal): eliminate odd rows
- Reduce (when more columns): find the first index in a row when next element is bigger, then go to next row and start from that index; eliminate all unindexed columns

Result of [6]

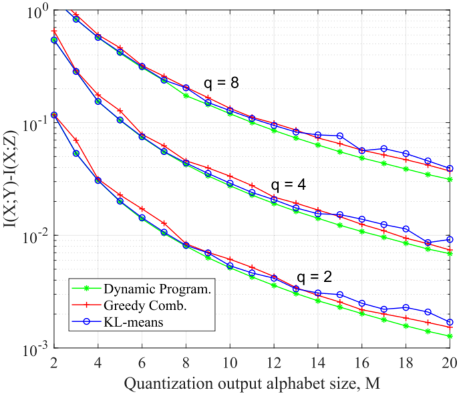

The DP design achieves global optimality with complexity $\mathcal{O}(q(N-M)M)$.

Table of Contents

Parameters

Table: Parameters in simulation

Transmit antenna Q	1
Tags K	2
States M	2
Reflect ratio α	0.5
Duration ratio N	10
Noise power σ_w^2	1
Discretization bins	256

Schemes

Input probability distribution schemes:

- Cooperation: assume full transmit cooperation (joint encoding) at all tags
- Exhaustion: evaluate and compare all possible input distributions
- KKT: solution by (10)
- Marginalization: marginalize the joint input array by Cooperation

Decision threshold schemes:

- SMAWK: aforementioned DP-based searching method [6]
- Bisection: sequentially optimizes each threshold by bisection [8]
- ML: requires no input distribution knowledge [9]

Results

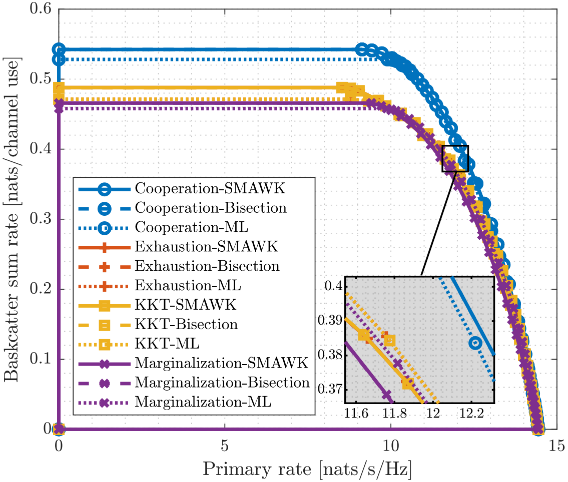

Figure: Achievable rate regions by input-threshold design: Case I.

Results

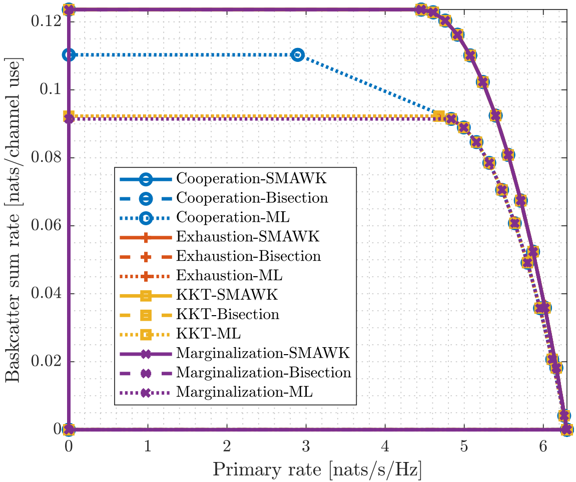

Figure: Achievable rate regions by input-threshold design: Case II.

W. Zhao, G. Wang, F. Gao, Y. Zou, and S. Atapattu, "Channel Capacity and Lower Bound for Ambient Backscatter Communication Systems," in *2017 9th International Conference on Wireless Communications and Signal Processing (WCSP)*, vol. 2017-Janua. IEEE, oct 2017, pp. 1–6. [Online]. Available: http://ieeexplore.ieee.org/document/8171133/

A. Raza, S. J. Nawaz, A. Ahmed, S. Wyne, B. Muhammad, M. N. Patwary, and R. Prasad, "A NOMA-Enabled Cellular Symbiotic Radio for mMTC," *Wireless Personal Communications*, vol. 122, no. 4, pp. 3545–3571, feb 2022. [Online]. Available: https://link.springer.com/10.1007/s11277-021-09100-z

Q. Wu and R. Zhang, "Towards Smart and Reconfigurable Environment: Intelligent Reflecting Surface Aided Wireless Network," *IEEE Communications Magazine*, vol. 58, no. 1, pp. 106–112, jan 2020. [Online]. Available: https://ieeexplore.ieee.org/document/8910627/

Y. Zhao, B. Clerckx, and Z. Feng, "IRS-Aided SWIPT: Joint Waveform, Active and Passive Beamforming Design under Nonlinear Harvester Model," *IEEE Transactions on Communications*, vol. 70, no. 2, pp. 1345–1359, 2022.

B. Molina-Farrugia, A. Rivadeneyra, J. Fernández-Salmerón, F. Martínez-Martí, J. Banqueri, and M. A. Carvajal, "Read Range Enhancement of a Sensing RFID Tag by Photovoltaic Panel," *Journal of Sensors*, vol. 2017, pp. 1–7, 2017. [Online]. Available: https://www.hindawi.com/journals/js/2017/7264703/

X. He, K. Cai, W. Song, and Z. Mei, "Dynamic Programming for Sequential Deterministic Quantization of Discrete Memoryless Channels," *IEEE Transactions on Communications*, vol. 69, no. 6, pp. 3638–3651, jun 2021. [Online]. Available: https://ieeexplore.ieee.org/document/9366549/

A. Aggarwal, M. M. Klawe, S. Moran, P. Shor, and R. Wilber, "Geometric Applications of a Matrix-Searching Algorithm," *Algorithmica*, vol. 2, no. 1-4, pp. 195–208, nov 1987. [Online]. Available: http://link.springer.com/10.1007/BF01840359

T. Nguyen and T. Nguyen, "On Thresholding Quantizer Design for Mutual Information Maximization: Optimal Structures and Algorithms," *IEEE Vehicular Technology Conference*, vol. 2020-May, 2020.

J. Qian, A. N. Parks, J. R. Smith, F. Gao, and S. Jin, "IoT Communications With M-PSK Modulated Ambient Backscatter: Algorithm, Analysis, and Implementation," *IEEE Internet of Things Journal*, vol. 6, no. 1, pp. 844–855, feb 2019. [Online]. Available: https://ieeexplore.ieee.org/document/8423609/